Molecular Systems Biology 3; Article number 131; doi:10.1038/msb4100171
Citation: ***Molecular Systems Biology*** **3:131**

www.molecularsystemsbiology.com

molecular systems biology

Dynamical modeling of syncytial mitotic cycles in *Drosophila* embryos

Laurence Calzone[1,2], Denis Thieffry[3], John J. Tyson[4] and Bela Novak[1,*]

[1] Molecular Network Dynamics Research Group of Hungarian Academy of Sciences and Budapest University of Technology and Economics, Budapest, Gellért tér, Hungary, [2] Institut Curie, Service de Bioinformatique, 26 rue d'Ulm, Paris, France, [3] INSERM ERM 206 & Université de la Méditerranée, Campus Scientifique de Luminy, Case 928,Marseille, France and [4] Department of Biological Sciences, Virginia Polytechnic Institute and State University, Blacksburg, VA, USA
* Corresponding author. Present address: Oxford Centre for Integrative Systems Biology, University of Oxford, South Parks Road, Oxford, OX1 3QU, UK.
Tel.: +44 1865275743; Fax: +44 1865275216; E-mail: bela.novak@bioch.ox.ac.uk

Received 8.1.07; accepted 22.6.07

Immediately following fertilization, the fruit fly embryo undergoes 13 rapid, synchronous, syncytial nuclear division cycles driven by maternal genes and proteins. During these mitotic cycles, there are barely detectable oscillations in the total level of B-type cyclins. In this paper, we propose a dynamical model for the molecular events underlying these early nuclear division cycles in *Drosophila*. The model distinguishes nuclear and cytoplasmic compartments of the embryo and permits exploration of a variety of rules for protein transport between the compartments. Numerical simulations reproduce the main features of wild-type mitotic cycles: patterns of protein accumulation and degradation, lengthening of later cycles, and arrest in interphase 14. The model is consistent with mutations that introduce subtle changes in the number of mitotic cycles before interphase arrest. Bifurcation analysis of the differential equations reveals the dependence of mitotic oscillations on cycle number, and how this dependence is altered by mutations. The model can be used to predict the phenotypes of novel mutations and effective ranges of the unmeasured rate constants and transport coefficients in the proposed mechanism.
Molecular Systems Biology 31 July 2007; doi:10.1038/msb4100171
Subject Categories: metabolic and regulatory networks; cell cycle
Keywords: cell cycle; cyclin B; *Drosophila* development; mathematical modeling; string

Introduction

During oogenesis, an egg grows very large and inherits from its mother all the nutrients and cell components needed to proceed through a series of cell cycles after fertilization (Wolpert, 2001). In many types of embryos, these early division cycles rapidly alternate between DNA replication (S-phase) and mitosis (M-phase). Later in development, the synchrony and speed of the first divisions is lost, and gap phases (G1 and G2) are introduced into the somatic cell cycle (Morgan, 2007).

The *Drosophila* egg is an extreme case. Its nuclei proceed through 13 very rapid (10–12 min) divisions without cell division. As a consequence, three hours following fertilization, 6000 nuclei share the same cytoplasm (syncytium). The rapidity of these early cycles can be explained by an abundance of maternally supplied cell cycle components. After mitosis 13, the nuclei become cellularized. Some cells arrest in G2, whereas other cells continue to divide at a slower and more variable schedule (Edgar and O'Farrell, 1990; Wolpert, 2001). The molecular basis of the first 13 rapid, synchronous nuclear division cycles is the subject of mathematical modeling in this paper.

The master regulators of the eukaryotic cell cycle are the cyclin-dependent protein kinases (Cdk's). To be active, a Cdk has to be associated with a cyclin partner, which determines the substrate specificity and subcellular localization of the Cdk/cyclin complex. The prototype of a Cdk/cyclin pair is M-phase-promoting factor (MPF), first identified in frog eggs. MPF is a complex of Cdk1 and a B-type cyclin (CycB). Cdk1 subunits are usually present in excess in cells, and therefore do not limit formation of Cdk/cyclin dimers. Cyclin subunits, on the other hand, fluctuate dramatically during the cell cycle and thereby play a major role in determining MPF activity (Morgan, 2007).

In growing cells, cyclin synthesis is regulated at the transcriptional level. In early embryonic cells, transcription is blocked or greatly restricted because they lack G1- and G2-phase (Morgan, 2007). In both growing and embryonic cells, cyclin level is controlled by proteolysis. Ubiquitylation of

CycB by the anaphase promoting complex (APC) targets them to the proteasome for degradation (Glotzer *et al*, 1991). In *Drosophila* embryos, a protein called Fzy (encoded by the *fizzy* gene) is responsible for targeting CycB to the APC during exit from mitosis (Dawson *et al*, 1995). The Fzy/APC complex is activated by phosphorylation by MPF (Peters, 2006), creating a negative-feedback loop (+/−) in the reaction network. The activation of Fzy/APC by MPF is an indirect process (Felix *et al*, 1990).

In addition, Cdk/cyclin activity can be controlled by phosphorylation of the Cdk subunit. Phosphorylation of a tyrosine residue (near the N terminus) inhibits the protein kinase activity of Cdk/cyclin complexes (the phosphorylated form of MPF, P-Cdk1/CycB, is called preMPF). Cdk phosphorylation is catalyzed by the protein kinase Wee1, and the phosphate group is removed by a phosphatase called String in *Drosophila* (Edgar and O'Farrell, 1990). Wee1 and String proteins are themselves phosphorylated by MPF, creating a pair of positive-feedback loops. String is activated by MPF (a +/+ loop) and Wee1 is inactivated by MPF (a −/− loop).

In sea urchin and frog embryos, the first 12 cell cycles are known to be driven by a cytoplasmic clock that causes periodic degradation of the CycB subunit of MPF as cells exit mitosis (Gerhart *et al*, 1984). The resultant oscillations of MPF activity control both nuclear divisions (M-phase) and the characteristic surface contractions that persist even after enucleation (Hara *et al*, 1980).

In contrast, in *Drosophila*, Edgar *et al* (1994b) observed that total CycB level and MPF activity remain high (not oscillating) during the first eight cycles. After cycle eight, small fluctuations appear in both CycB level and MPF activity with increasing amplitude. Even though CycB degradation might appear negligible during these early cycles, introduction of a nondegradable form of CycB into a *Drosophila* embryo blocks mitotic cycles, which underlines the importance of CycB degradation at certain stages of the cell cycle (Su *et al*, 1998; Raff *et al*, 2002).

The apparent paradox surrounding CycB degradation during *Drosophila* embryogenesis can be resolved by recognizing that CycB degradation occurs only locally, in the vicinity of the mitotic spindle (Huang and Raff, 2002; Raff *et al*, 2002). In this paper, we use mathematical modeling to explore whether the hypothesis of local CycB degradation gives an adequate description of CycB patterns during the first 13 nuclear division cycles of the *Drosophila* embryo. After introducing compartmentalization and local degradation, we show that it is possible to simulate the key features of early embryonic cell cycles in *Drosophila*. The model also reproduces the effects of alpha-amanitin treatment, loss-of-function mutations and overexpression mutations.

Results

A model for the molecular network controlling embryonic cell cycles in *Drosophila*

Our model for cell cycle regulation in the early *Drosophila* embryo, inspired by Figure 7 of Edgar *et al* (1994b), is diagrammed in full in Figure 1A. The model tracks the interactions of MPF, Fzy, Wee1 and String in the cytoplasm

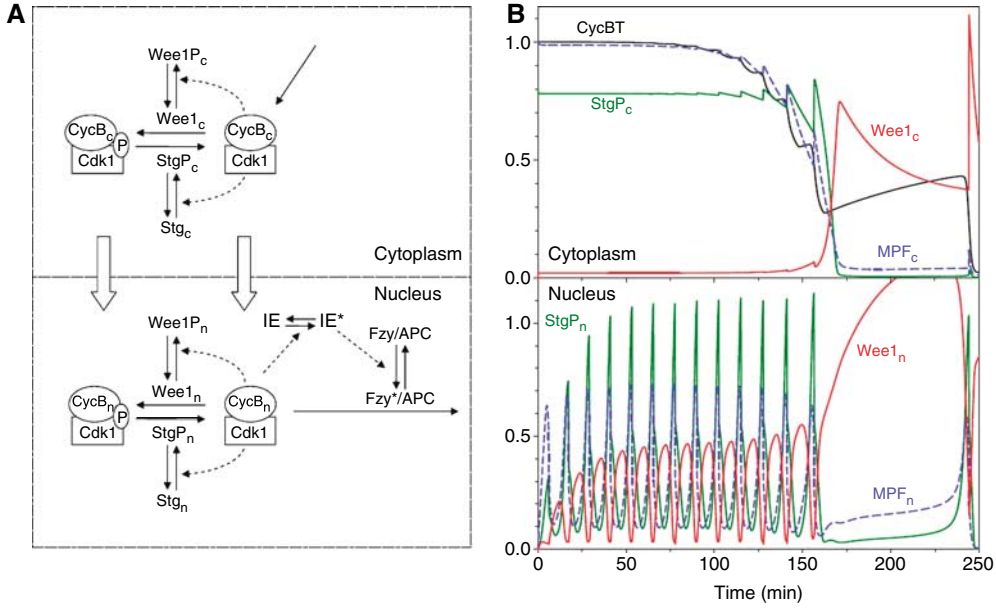

Figure 1 Dynamical model of nuclear division cycles during early embryogenesis of *Drosophila*. (**A**) Two compartments are considered: nuclei and cytoplasm. MPF (Cdk1/CycB), Wee1 and String (Stg) are present in both compartments and can move between the compartments. These three components can exist in phosphorylated and unphosphorylated forms (P-Cdk1/CycB is called preMPF). Fzy is present only in the nucleus, in the vicinity of the mitotic spindle, where it assists the APC in labeling CycB subunits for degradation. Fzy is activated (Fzy*) by nuclear MPF through an intermediary enzyme (IE). In the cytoplasm, MPF$_c$ and preMPF$_c$ are degraded at a constant low rate (reactions not shown). The reaction network is similar to a model of frog egg division cycles (Novak and Tyson, 1993), except that CycB degradation is here limited to the nuclear compartment. (**B**) Temporal evolution of protein concentrations. The total amounts of String and Wee1 are constant (0.8 each) in this simulation. Fourteen oscillations driven by MPF$_n$ precede the G2 arrest. For this simulation, we set k_{sstg} and k_{dstg} equal to 0, and the initial values for MPFc, StgPc and Wee1Pc to 1, 0.8 and 0.8, respectively.

and in the nuclei. In *Drosophila*, Fzy/APC is localized at centrosomes, kinetochores and spindles (Su *et al*, 1998; Huang and Raff, 1999; Raff *et al*, 2002). Consequently, we assume that CycB subunits of MPF undergo regulated destruction only in the nuclear compartments. In our model, MPF activates Fzy/APC through an 'intermediary enzyme' (IE), because some evidence indicates that the activation step is indirect (Felix *et al*, 1990). These interactions comprise a delayed negative-feedback loop that generates local oscillations of MPF activity in the nuclear compartments. Meanwhile, Wee1 and String are also regulating MPF activity in both compartments by phosphorylating and dephosphorylating (respectively) a tyrosine residue on the Cdk subunit of MPF.

Using the basic principles of biochemical kinetics, we translate the diagram into a set of ordinary differential equations (Table I). The equations, which describe the time-rates of change of the fluctuating protein species in the diagram, contain a number of unknown rate constants that must be estimated by fitting the model to the available data (mutant phenotypes, responses to drug treatments, and so on). The parameter values reported in Table II are suitable for simulating the experiments described in this paper.

Modeling localized cyclin degradation

We distinguish two compartments in the embryo (Figure 1A): cytoplasm and nuclei. What we call the 'nuclear compartment' is not the volume enclosed by the nuclear envelope, because the nuclear envelope breaks down during mitosis. Despite the loss of a barrier between nucleus and cytoplasm, we assume that CycB degradation during M-phase occurs only in a limited region (our 'nuclear compartment') in the vicinity of the mitotic spindle. Hence, in our model, the nuclear compartment persists in separation from the cytoplasmic compartment throughout the nuclear division cycles. At telophase, the number of nuclear compartments doubles (or, nearly so), as described later. We will assume that the transport coefficients for MPF, Wee1 and String between nucleus and cytoplasm do not change as the nuclear envelope breaks down and reassembles each cycle. In the Discussion, we will present evidence that our conclusions are not significantly changed by the more likely assumption that intercompartmental transport increases during mitosis.

The volume of the nuclear compartment is assumed to be the product of the number of nuclei (N) and the volume of a single nuclear compartment (V_n), that is $V_N=NV_n$. Consequently, cytoplasmic volume is $V_C=V_T(1-N\varepsilon)$, where $V_T=$ total egg volume (constant) and $\varepsilon=V_n/V_T \ll 1$.

Next, we need to specify how individual proteins are distributed between nuclei and cytoplasm. For example, MPF is present in both cytoplasm and nuclei, where its concentrations are denoted $[MPF_c]$ and $[MPF_n]$, respectively. The average concentration of MPF across the entire cell is given by

$$[MPF]_T = \frac{[MPF_c]V_C + N[MPF_n]V_n}{V_T} = (1-N\varepsilon)[MPF_c] + N\varepsilon[MPF_n]$$

The balance equations for transport of MPF between cytoplasm and nucleus are

$$\left(\frac{d[MPF_c]}{dt}\right)_{transport} = \frac{N(J_{out}-J_{in})}{V_C}, \left(\frac{d[MPF_n]}{dt}\right)_{transport} = \frac{J_{in}-J_{out}}{V_n}$$

where J_{in} and J_{out} are the fluxes of MPF (number of molecules per unit time) into and out of a single nucleus. We assume that $J_{in}=A_nP_{in}[MPF_c]$ and $J_{out}=A_nP_{out}[MPF_n]$, where P_{in} and P_{out} are permeability constants and A_n is the surface area of a single nucleus (assumed constant). Defining first-order rate constants, $k_{in}=A_nP_{in}/V_T$ and $k_{out}=A_nP_{out}/V_T$, we can write the transport laws as

$$\left(\frac{d[MPF_c]}{dt}\right)_{transport} = \frac{N}{1-N\varepsilon}(k_{out}[MPF_n] - k_{in}[MPF_c]),$$

$$\left(\frac{d[MPF_n]}{dt}\right)_{transport} = \frac{1}{\varepsilon}(k_{in}[MPF_c] - k_{out}[MPF_n]).$$

For proteins that are actively accumulated in nuclei, $k_{in} \gg k_{out}$.

The balance equations for MPF_c and MPF_n can now be written as

$$\frac{d[MPF_c]}{dt} = \frac{N}{1-N\varepsilon}(OUT - IN) + SYN - DEG - KIN + PHOS,$$

$$\frac{d[MPF_n]}{dt} = \frac{1}{\varepsilon}(IN - OUT) - DEG - KIN + PHOS$$

where IN, OUT, SYN, and so on stand for the rate expressions for transport and chemical reactions. Similar equations hold for preMPF. For MPF and preMPF, we assume that $k_{out}=0$.

Wee1 and String are also distributed between cytoplasm and nuclei, and these proteins can be phosphorylated and dephosphorylated in both compartments. As a consequence, we consider four different forms of each protein (unphosphorylated and phosphorylated forms in the cytoplasm and in the nuclei), where the cytoplasmic forms (Stg_c, $StgP_c$, $Wee1_c$ and $Wee1P_c$) interact with MPF_c and $preMPF_c$, whereas the nuclear forms (Stg_n, $StgP_n$, $Wee1_n$ and $Wee1P_n$) interact with MPF_n and $preMPF_n$. For String and Wee1, we can write balance equations for the total concentrations:

$$[String]_T = (1-N\varepsilon)([Stg_c]+[StgP_c]) + N\varepsilon([Stg_n]+[StgP_n])$$
$$[Wee1]_T = (1-N\varepsilon)([Wee1_c]+[Wee1P_c]) + N\varepsilon([Wee1_n] + [Wee1P_n])$$

In some figures we plot the total concentration of phosphorylated String, given by:

$$[Stg\_Phospho] = (1-N\varepsilon)[StgP_c] + N\varepsilon[StgP_n]$$

By assumption $[Wee1]_T$ is constant in the model, so we can compute $Wee1P_c$ from the equation:

$$[Wee1P_c] = \frac{[Wee1]_T - N\varepsilon([Wee1_n]+[Wee1P_n])}{1-N\varepsilon} - [Wee1_c]$$

In the model, we assume that nuclei enter M-phase when MPF_n activity abruptly increases, and they divide when MPF_n activates Fzy/APC (i.e., when Fzy activity increases through 0.5). At each cycle, the N nominally doubles. However, to

Table I Equations of the complete *Drosophila* model

$$\frac{d[MPF_n]}{dt} = k_{in}[MPF_c] - k_{out}[MPF_n] - (k'_{d,n} + k''_{d,n}[FZY])[MPF_n] - (k'_{wee} + k''_{wee}[Wee1_n])[MPF_n] + (k'_{stg} + k''_{stg}[StgP_n])[preMPF_n] \quad (1)$$

$$\frac{d[preMPF_n]}{dt} = k_{in}[preMPF_c] - k_{out}[preMPF_n] - (k'_{d,n} + k''_{d,n}[FZY])[preMPF_n] + (k'_{wee} + k''_{wee}[Wee1_n])[MPF_n] - (k'_{stg} + k''_{stg}[StgP_n])[preMPF_n] \quad (2)$$

$$\frac{d[MPF_c]}{dt} = k_{s,c} - k'_{d,c}[MPF_c] - \frac{N\varepsilon}{1-N\varepsilon}(k_{in}[MPF_c] - k_{out}[MPF_n]) - (k'_{wee} + k''_{wee}[Wee1_c])[MPF_c] + (k'_{stg} + k''_{stg}[StgP_c])[preMPF_c] \quad (3)$$

$$\frac{d[preMPF_c]}{dt} = -k'_{d,c}[preMPF_c] - \frac{N\varepsilon}{1-N\varepsilon}(k_{in}[preMPF_c] - k_{out}[preMPF_n]) + (k'_{wee} + k''_{wee}[Wee1_c])[MPF_c] - (k'_{stg} + k''_{stg}[StgP_c])[preMPF_c] \quad (4)$$

$$\frac{d[IE]}{dt} = \frac{k_{a,ie}[MPF_n](1-[IE])}{J_{a,ie} + 1 - [IE]} - \frac{k_{i,ie}[IE]}{J_{i,ie} + [IE]} \quad (5)$$

$$\frac{d[FZY]}{dt} = \frac{k_{a,fzy}[IE](1-[FZY])}{J_{a,fzy} + 1 - [FZY]} - \frac{k_{i,fzy}[FZY]}{J_{i,fzy} + [FZY]} \quad (6)$$

$$\frac{d[StgP_n]}{dt} = k_{in,s}[StgP_c] - k_{out,s}[StgP_n] - k_{d,stg}[StgP_n] + \frac{(k'_{a,stg} + k''_{a,stg}[MPF_n]) \cdot [Stg_n]}{J_{a,stg} + [Stg_n]} - \frac{k_{i,stg}[StgP_n]}{J_{i,stg} + [StgP_n]} \quad (7)$$

$$\frac{d[Stg_n]}{dt} = k_{in,s}[Stg_c] - k_{out,s}[Stg_n] - k_{d,stg}[Stg_n] - \frac{(k'_{a,stg} + k''_{a,stg}[MPF_n])[Stg_n]}{J_{a,stg} + [Stg_n]} + \frac{k_{i,stg}[StgP_n]}{J_{i,stg} + [StgP_n]} \quad (8)$$

$$\frac{d[StgP_c]}{dt} = -k_{d,stg}[StgP_c] - \frac{N\varepsilon}{1-N\varepsilon}(k_{in,s}[StgP_c] - k_{out,s}[StgP_n]) + \frac{(k'_{a,stg} + k''_{a,stg}[MPF_c])[Stg_c]}{J_{a,stg} + [Stg_c]} - \frac{k_{i,stg}[StgP_c]}{J_{i,stg} + [StgP_c]} \quad (9)$$

$$\frac{d[Stg_c]}{dt} = k_{s,stg}[Stgm] - k_{d,stg}[Stg_c] - \frac{N\varepsilon}{1-N\varepsilon}(k_{in,s}[Stg_c] - k_{out,s}[Stg_n]) - \frac{(k'_{a,stg} + k''_{a,stg}[MPF_c])[Stg_c]}{J_{a,stg} + [Stg_c]} + \frac{k_{i,stg} \cdot [StgP_c]}{J_{i,stg} + [StgP_c]} \quad (10)$$

$$\frac{d[Wee1P_n]}{dt} = k_{in,w}[Wee1P_c] - k_{out,w}[Wee1P_n] - \frac{k_{a,wee}[Wee1P_n]}{J_{a,wee} + [Wee1P_n]} + \frac{(k'_{i,wee} + k''_{i,wee}[MPF_n])[Wee1_n]}{J_{i,wee} + [Wee1_n]} \quad (11)$$

$$\frac{d[Wee1_n]}{dt} = k_{in,w}[Wee1_c] - k_{out,w}[Wee1_n] + \frac{k_{a,wee}[Wee1P_n]}{J_{a,wee} + [Wee1P_n]} - \frac{(k'_{i,wee} + k''_{i,wee}[MPF_n])[Wee1_n]}{J_{i,wee} + [Wee1_n]} \quad (12)$$

$$\frac{d[Wee1_c]}{dt} = -\frac{N\varepsilon}{1-N\varepsilon}(k_{in,w}[Wee1_c] - k_{out,w}[Wee1_n]) + \frac{k_{a,wee}[Wee1P_c]}{J_{a,wee} + [Wee1P_c]} - \frac{(k'_{i,wee} + k''_{i,wee}[MPF_c])[Wee1_c]}{J_{i,wee} + [Wee1_c]} \quad (13)$$

$$\frac{d[Stgm]}{dt} = -\left(\frac{k'_{d,m}}{J_m + [Stgm]} + k''_{d,m}[Xp]\right)[Stgm] \quad (14)$$

$$\frac{d[Xm]}{dt} = k_{s,xm}N \quad (15)$$

$$\frac{d[Xp]}{dt} = k_{s,xp}[Xm] \quad (16)$$

$$[CycB]_T = (1-N\varepsilon)([MPF_c] + [preMPF_c]) + N\varepsilon([MPF_n] + [preMPF_n]) \quad (17)$$

$$[String]_T = (1-N\varepsilon)([Stg_c] + [StgP_c]) + N\varepsilon([Stg_n] + [StgP_n]) \quad (18)$$

$$[Wee1P_c] = \frac{[Wee1]_T - N\varepsilon([Wee1_n] + [Wee1P_n])}{1-N\varepsilon} - [Wee1_c] \quad (19)$$

$$Stg\_Phospho = (1-N\varepsilon)[StgP_c] + N\varepsilon[StgP_n] \quad (20)$$

When Fzy=K_{ez} (increasing), then the following changes are made instantaneously (for X=MPF, preMPF, Wee1, Wee1P, Stg, and StgP):

$$X_c \to \frac{1-N\varepsilon}{1-1.95N\varepsilon}X_c, \quad X_n \to \frac{X_n}{1.95}, \quad N \to 1.95N$$

account for the few nuclei that do not divide, we multiply the existing N at each division by 1.95 rather than by 2.

If we assume that the concentrations of protein species do not change at the point of discontinuity (when N increases to 1.95 N), then there is a sudden 'creation of matter' needed to populate the new nuclei with all their protein components. For proteins that turn over (synthesis and degradation), this new material is quickly equilibrated and the excess removed by

Table II Parameter values for the equations in Table I

(Rate constants, min^{-1})					
$k_{s,c} = 0.01$	$k_{d,c}' = 0.01$	$k_{d,n}' = 0.01$	$k_{d,n}'' = 1.5$	$k_{a,ie} = 1$	$k_{i,ie} = 0.4$
$k_{a,fzy} = 1$	$k_{i,fzy} = 0.2$	$k_{wee}' = 0.005$	$k_{wee}'' = 1$	$k_{stg}' = 0.2$	$k_{stg}'' = 2$
$k_{s,xm} = 0.0005$	$k_{s,xp} = 0.001$	$k_{d,m}' = 0.002$	$k_{d,m}''0.2$	$k_{s,stg} = 0.02$	$k_{d,stg} = 0.015$
$k_{a,stg}' = 0$	$k_{a,stg}'' = 1$	$k_{i,stg} = 0.3$	$k_{a,wee} = 0.3$	$k_{i,wee}' = 0.01$	$k_{i,wee}'' = 1$
$k_{in} = 0.15$	$k_{out} = 0$	$k_{in,s} = 0.08$	$k_{out,s} = 0.02$	$k_{in,w} = 0.04$	$k_{out,w} = 0.01$
(Dimensionless parameters)					
$\varepsilon = 0.00007$	$J_{a,ie} = 0.01$	$J_{i,ie} = 0.01$	$J_{a,fzy} = 0.01$	$J_{i,fzy} = 0.01$	$J_{a,stg} = 0.05$
$J_{i,stg} = 0.05$	$J_{a,wee} = 0.05$	$J_{i,wee} = 0.05$	$J_m = 0.05$	$k_{ez} = 0.5$	$[Wee1]_T = 0.8$

protein degradation, with no appreciable effect on the solution of the differential equations during the 13 cycles. But for conserved species (e.g., Wee1), there is a steady increase of total concentration, as a little new material is created at each division. The increase starts to become noticeable at the 12th division. The problem can be remedied by rescaling concentrations after nuclear division according to the prescriptions (see Materials and methods section for details):

$$X_{n\_after} \rightarrow \frac{1}{1.95} X_{n\_before}$$

(nuclear concentrations diluted at division)

$$X_{c\_after} \rightarrow \frac{1 - N\varepsilon}{1 - 1.95N\varepsilon} X_{c\_before}$$

(cytoplasmic concentrations slightly increased)

Figure 1B shows the results of a numerical simulation of the model with localized cyclin degradation. For this simulation, we assume no synthesis or degradation of String, that is, $[String]_T$=constant. The initial concentration for MPF in the cytoplasm is high (one arbitrary unit) and this activity suffices to keep Wee1 inactive and String active in the cytoplasm (at least initially). The first oscillations of the nuclear concentration of MPF are very rapid. However, in later cycles, they slow down, and finally arrest in G2-phase of the 15th cycle with low MPF activity. The first 13 cycles are so rapid in *Drosophila* compared to *Xenopus*, because they are driven by nuclear import of pre-formed cytoplasmic CycB rather than by *de novo* synthesis of CycB. In the early cycles, MPF enters the nucleus so quickly that nuclear Wee1 cannot inhibit it and, as a result, the rapid accumulation of MPF_n drives the nucleus into mitosis. These early cycles are driven by the negative-feedback circuit involving MPF_n, IE and Fzy/APC.

As the *N* and the volume of the nuclear compartment nearly double after each mitosis, the concentration of MPF + preMPF in the cytoplasm decreases. The drop in the cytoplasmic concentration slows down the transport of MPF into the nuclei and thus slows down the oscillation. As Wee1 kinase activity in the nucleus becomes more and more comparable to the nuclear entry rate of MPF, MPF complexes can be inhibited through tyrosine phosphorylation by Wee1. MPF_n activity must reach a certain threshold to switch Wee1 kinase off and to activate String. As reaching this threshold takes some time, the period of the oscillation increases further. Eventually, total cyclin level in the cytoplasm is so low that nuclear MPF concentration cannot surmount the threshold level to enter mitosis. Hence, Wee1 remains active and String inactive, and MPF oscillations cease. In Figure 1B, the 'embryo' has an extended cycle 14 and arrests in cycle 15. (The cycle number (*C*) for which the model arrests depends sensitively on parameter values.)

Probing the regulatory mechanism and parameter constraints at the origin of cellular oscillations

In this section, we use one-parameter bifurcation diagrams to characterize the mitotic control system with localized cyclin degradation (Tyson *et al*, 2002; Csikasz-Nagy *et al*, 2006). A bifurcation diagram describes the stability of a dynamical system as some key parameter (the *bifurcation* parameter) is changed. As bifurcation parameter, we introduce 'cycle number' *C*, defined by N=1.95^{C-1}. With this definition, *N* is the number of nuclei in the egg during cycle number *C*. When computing a bifurcation diagram, *C* is treated as a real number, even though *N* increases stepwise during simulations. For the bifurcation diagrams in Figure 2, the state of the control system (on the vertical axis) is characterized by either nuclear MPF or total CycB (to give two different views of system state).

For a large *N*, the control system has a single, stable steady state (solid line) with low MPF_n concentration. At this steady state, MPF is tyrosine phosphorylated both in the cytoplasm and in the nuclei. This stable steady state represents a G2 arrest. When *N* is small, the control system is in a region where a branch of unstable steady states (dashed line) is surrounded by stable limit cycle oscillations (filled circles). These oscillations have large amplitude of $[MPF]_n$, but small amplitude of $[CycB]_T$ (Figure 2A). As *N* increases after every oscillation, we move from left to right (*C* increasing) on the bifurcation diagram as the embryo develops.

Between cycles 11 and 12 (Figure 2A), the limit cycle oscillations undergo a pair of 'cyclic fold' bifurcations, which indicate a qualitative change in the oscillation mechanism. For $C \leqslant 11$, the oscillations are driven by the negative-feedback loop (cyclin degradation) alone. For $C \geqslant 12$, the positive-feedback loops (involving MPF phosphorylation) contribute to the oscillatory mechanism. These positive-feedback loops become more and more significant as *C* increases, eventually creating alternative stable steady states between cycles 14 and 15. The stable steady state with low activity of MPF_n blocks the oscillations at a SNIC bifurcation (saddle-node-invariant-circle, where the period of oscillation tends toward infinity) at C=14.33. Hence, the MPF control system completes cycle 14 and arrests at a stable steady state in interphase of cycle 15.

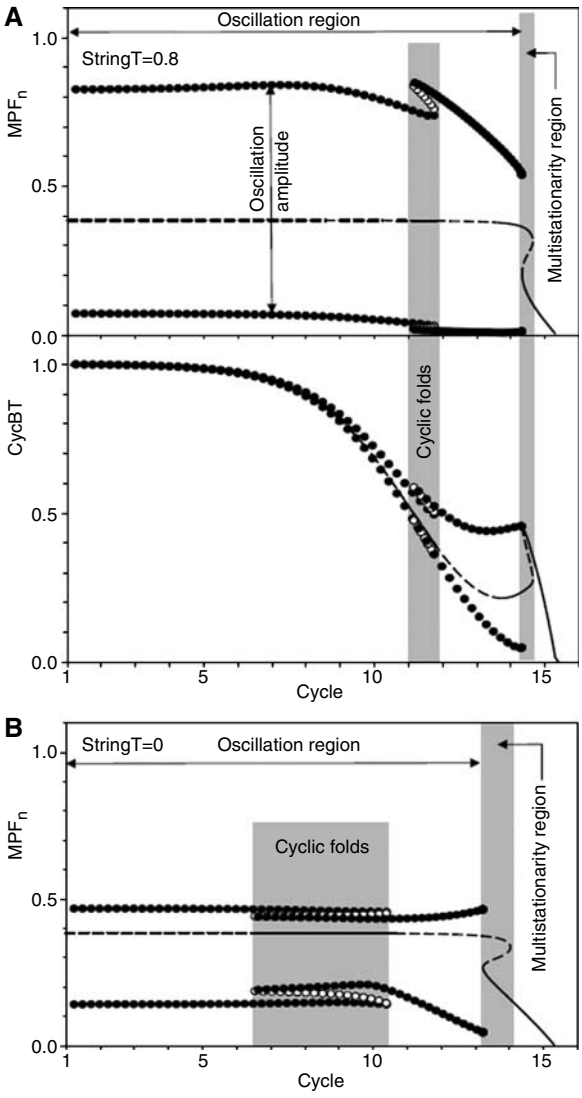

Figure 2 Bifurcation diagrams. Dashed lines represent unstable steady states and solid lines represent stable steady states. The small circles trace the maximum and minimum excursions of the state-variable during limit cycle oscillations. Filled and empty circles indicate stable and unstable limit cycles, respectively. (**A**) MPF_n activity and CycBT (the total concentration of cyclin in both compartments) are plotted as a function of C for StringT= 0.8. MPF_n shows stable limit-cycle oscillations (around an unstable steady state) with varying amplitude for 14 cycles, then the system arrests on a branch of stable steady states. (**B**) MPF_n activity versus C for StringT=0. Compared to (A), the SNIC bifurcation point is moved from cycle 14 to 13.

This is a problem, because *Drosophila* eggs arrest in interphase of cycle 14. It could be corrected by adjusting some parameters to move the SNIC point to $13 < C < 14$, but there are other more serious problems to be solved, along with this one, in the next section.

Interestingly, the bifurcation diagram does not change very much in the absence of String (Figure 2B), that is, a maternal *string* loss-of-function mutation. The reason for this insensitivity is the existence of a second protein phosphatase, Twine, which overlaps the function of String (Edgar and Datar, 1996). (Twine activity is represented in the model by the parameter k_{stg}'.) In the absence of String, the amplitude of MPF_n oscillations is slightly reduced, and the SNIC bifurcation point moves to a slightly smaller value of C (=13.22). Consequently, MPF_n oscillations stop one cycle earlier (in cycle 14) than for $[String]_T$=0.8.

Including String synthesis and degradation

Although the simulation in Figure 1B is superficially similar to observations of MPF fluctuations in fruit fly embryos (Edgar *et al*, 1994b), there are significant quantitative differences: (1) the number of division cycles is incorrect (easily fixed), and (2) the total amount of String in the embryo is not constant (less easily fixed). String protein level in embryos is low at fertilization, rises for seven or eight cycles and drops gradually to zero at interphase 14. As String level determines the position of the SNIC bifurcation (where oscillations are suppressed), we need to extend the model to changing levels of String protein. To this end, we take into account that *string* mRNA is stable until cycle 14 and is degraded abruptly in the first 20 min of interphase 14 (Edgar *et al*, 1994a).

Two distinct mechanisms seem to be responsible for *string* mRNA degradation (Edgar and Datar, 1996; Bashirullah *et al*, 1999), one operating on maternal *string* mRNA and the other one mediated by zygotically induced genes. To describe String dynamics, we append to the model (Table I) three differential equations: for *string* mRNA (equation (14)), for the mRNA of an unknown factor X (equation (15)) that is responsible for degrading *string* mRNA, and for the corresponding protein level (equation (16)). We assume that X_m (mRNA for factor X) is synthesized in the embryo at a rate proportional to N. The protein X_p is produced at a rate proportional to X_m. The rate constants in equations (15) and (16) are chosen so that there is no detectable synthesis of X_p until about the 10th cycle, and then its level rises sharply in cycles 11–13. (Other assumptions might be more reasonable: for example, X_m may not be synthesized during the very rapid cycles 1–6, when the DNA is likely unavailable for transcription. In that case, the rate constants would have to be readjusted to maintain the sharp rise in X_p in cycles 11–13.)

We assume that the *string* gene is not transcribed during early embryonic cycles, so the differential equation for *string* mRNA (equation (14)) has only degradation terms. The first term represents degradation by maternal products, whereas the second term is degradation by X_p. Hence, String message level drops slowly at first and then increasingly faster in cycles 11–13. String protein is assumed to be synthesized at a rate proportional to its mRNA (Stg_m) and degraded with first order kinetics. Hence, total String protein level rises during the first 9–10 cycles and then decays away after its message is destroyed.

With these amendments to the model, a better description of the early cell cycles in *Drosophila* is achieved (Figure 3). The levels of String message and protein change as observed in Edgar's experiments (Edgar and Datar, 1996) and the embryo arrests solidly in interphase of cycle 14. In the simulation (Figure 3C), oscillations in String phosphorylation become noticeable around cycle 8, whereas, in experiments, fluctuations in String phosphorylation are already observed in cycle 5 or 6 (Edgar *et al*, 1994b).

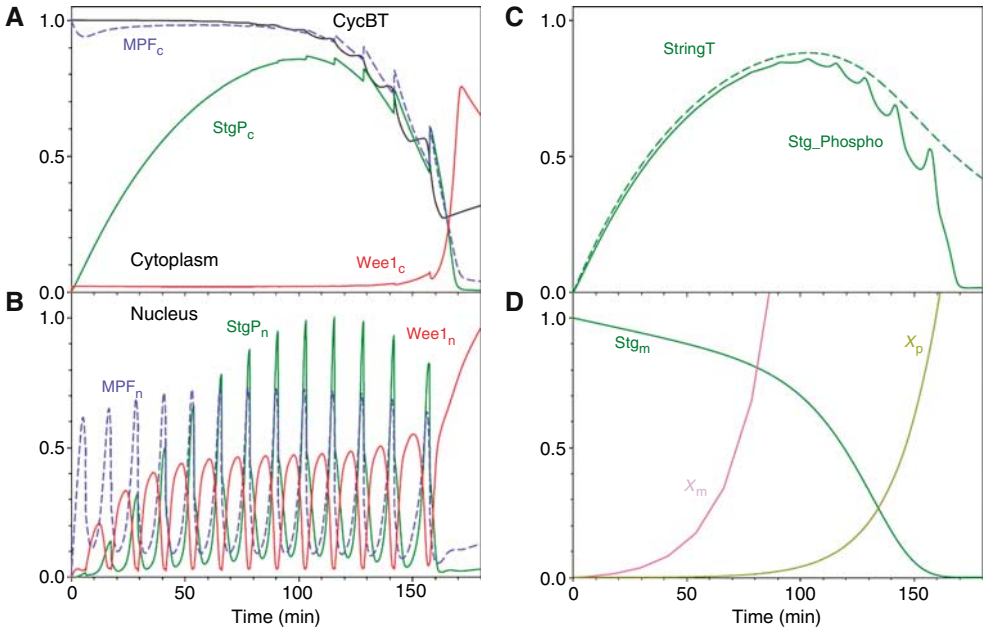

Figure 3 Time-courses of protein concentration, for the case where StringT is not constant. (**A**) Concentrations of cytoplasmic MPF, Wee1 and String, along with the total amount of CycB. (**B**) The same proteins acting in the nuclei. (**C**) Total concentration of String protein in the cell, along with the total concentration of phosphorylated String. (**D**) Dynamics of maternal *string* mRNA (Stg_m) and the message and protein levels of 'factor X' (X_m and X_p).

Table III Observed and simulated phenotype of *Drosophila* cell cycle mutants

Parameter change	Simulation result	Genotype	Phenotype	Reference
$k_{dn}'' = 0$	Arrest in metaphase	fzyΔ or CycBdbΔ	Arrest in metaphase	Dawson *et al* (1993); Su *et al* (1998)
$k_{dn}'' = 0.75$	13 cycles	1 × fzy	—	—
$k_{dn}'' = 3.0$	Fast 14 cycles	4 × fzy	—	—
$k_{sc} = 0.007$, init $MPC_c = 0.7$	Delay in late cycles	1 × CycB	Delays in cycles 10–13	Crest *et al* (2007); Ji *et al* (2004)
$k_{sc} = 0.015$ init $MPC_c = 1.5$	Interphase arrest in cycle 15	4 × CycB	One extra nuclear division	Crest *et al* (2007); Ji *et al* (2004)
$k_{stg}'' = 0$	13 cycles	2 × twn 0 × stg	Arrest in 14th cycle	Edgar and Datar (1996)
$k_{stg}'' = 0$, $k_{stg}' = 0.15$	12 cycles	1 × twn 0 × stg	One cycle less	Edgar and Datar (1996)
$k_{stg}'' = 0$, $k_{stg}' = 0$	No cycles	0 × twn 0 × stg	—	Edgar and Datar (1996)
$k_{stg}' = 1.2$	Extra MPF cycle	6 × twn	Few extra nuclear cycles	Edgar and Datar (1996)
$Stg_m = 2$	Extra MPF cycle	4 × Stg	13 normal cycles	Edgar and Datar (1996)
$Wee1_{tot} = 2.4$	12 cycles	6 × Wee1	—	—
$k_{wee}'' = 0$	Fast 13 cycles	0 × Wee1	Fast cycle	Stumpff *et al* (2004)

Simulation of gene dosage effects

If this model is basically correct, it should account not only for all features of nuclear division in wild-type embryos, but also for subtle differences in phenotypes of mutant embryos. In this case, the relevant mutants are deletions and overexpressions of *cycB*, *fizzy*, *wee1*, *string* and *twine*. Simulations of these mutants are summarized in Table III.

Deletion of *fizzy* breaks the negative-feedback loop on which the oscillations depend and is, of course, lethal to embryonic development (Dawson *et al*, 1993). The model predicts that a half-dose of *fizzy* (*fizzy*$^{+/-}$ heterozygote) is similar to wild type, whereas overexpressing *fizzy* may produce an extra nuclear division. Overexpressing *cycB* speeds up the cycles and adds an extra nuclear division (Ji *et al*, 2004; Crest *et al*, 2007). Conversely, a half-dose of *cycB* causes delays in cycles 10–13 (Ji *et al*, 2004; Crest *et al*, 2007).

Deletion of *string* has no effect on the early mitotic cycles, as long as *twine* is in place (see Figure 2B: *string* deletion halts in cycle 14), but deletion of both genes is lethal to the egg (Edgar and Datar, 1996). Interestingly, deletion of *string* and a half-dose of *twine* cause the early cycles to stop one division earlier than normal (in cycle 13) in the model and in experiments (Edgar and Datar, 1996). In the bifurcation diagram for this mutant, the SNIC bifurcation is moved to C=12.57 (i.e., the egg arrests in cycle 13).

Overexpressing *string* and/or *twine* is tricky to interpret. We might expect such mutations to speed up the cycles and perhaps add an extra nuclear division (arrest in cycle 15). An extra division is observed in a small fraction (3–5%) of embryos (Edgar and Datar, 1996). In simulations, extra peaks of MPF_n are observed, but the later cycles are of reduced amplitude and it is not clear whether they could effectively drive a complete mitosis or not. The reason for the reduction in

amplitude of MPF_n oscillations is clear from the bifurcation diagram (Supplementary Figure S1). The SNIC bifurcation is lost and the later oscillations arise from a supercritical Hopf bifurcation (small amplitude limit cycle oscillations). The bifurcations in this case can be very complex, but the end result in simulations is a damped oscillation of MPF_n.

The *wee1* gene is not essential for early nuclear divisions (Stumpff *et al*, 2004). In simulations, the *wee1*-deletion mutant (like *twine* and *string* overexpression mutants) arrests via damped oscillations at a supercritical Hopf bifurcation (Supplementary Figure S2). Simulation of a *wee1*-overexpressing mutant ($6 \times$ *wee1*) predicts nuclear-division arrest in cycle 12 (Table III).

Simulation of the effects of alpha-amanitin treatment

Edgar and Datar (1996) showed that if an embryo is treated before cycle 6 with alpha-amanitin (an inhibitor of RNA polymerase), then 88% of the nuclei arrest at interphase of cycle 15 instead of cycle 14. If the same treatment is performed later, then the extra cycle is not observed (Myers *et al*, 1995; Edgar and Datar, 1996). These results are nicely reproduced by simulations. In Figure 4A, we let the model run up to t=55 min (just before cycle 6), then set $k_{s,xm}$=0 (i.e., no further synthesis of X message), then continue the simulation. The concentration of X_p never gets very large, and the degradation of *string* mRNA is slower. As a result, total String protein is slightly higher, allowing an extra cycle to occur. In contrast, when we simulate the same treatment at t=75 min (after cycle 6), X_p concentration is higher, *string* mRNA drops faster and no extra cycle is observed.

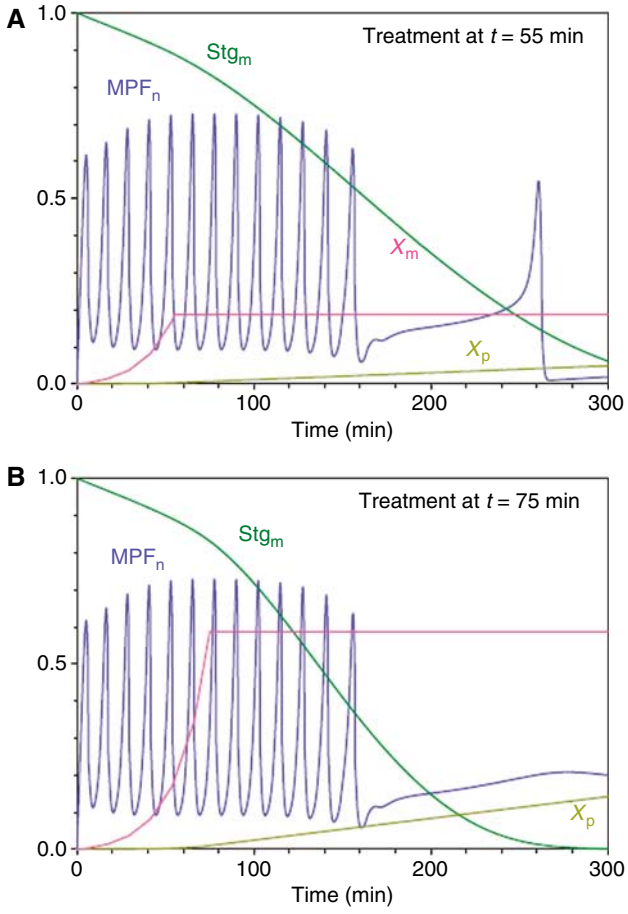

Figure 4 Simulation of alpha-amanitin treatments. (**A**) The simulation is run for 55 min (before cycle 6) in normal conditions, then $k_{s,m}$ is set to 0 (i.e., transcription of factor X is blocked by alpha-amanitin), then the simulation is continued. (**B**) Same as (A), but the block is imposed after cycle 6.

Discussion

Early development of *Drosophila* embryos has been thoroughly studied by developmental geneticists and molecular biologists. Prompted by beautiful data on gene expression patterns, many groups have proposed models for pattern formation in post-blastoderm embryos (von Dassow *et al*, 2000; Sanchez and Thieffry, 2003; Jaeger *et al*, 2004). Until now, however, no one has systematically explored the role of protein interactions during the first 13 nuclear division cycles in the syncytial, undifferentiated embryo. These cycles are remarkable because of their great speed (approx 10 min cycle time) and because they are not associated with large changes in observable activity of MPF, as seen for example in the embryos of sea urchins and frogs.

Although the bulk cytoplasm of the syncytial *Drosophila* egg contains a massive amount of active MPF, the activity of MPF in the vicinity of chromosomes may fluctuate dramatically, first of all because active MPF must be imported into the nuclei during interphase, and secondly because MPF activity may be cleared from chromosomal regions by rapid CycB degradation on anaphase spindles. Many authors have previously forwarded this hypothesis, or something similar, to explain the curious features of nuclear division in the early embryo of *Drosophila* (Edgar *et al*, 1994b; Crest *et al*, 2007). We have explored this hypothesis in terms of a mathematical model that distinguishes nuclear compartments from the bulk cytoplasm. Nuclear import of active MPF drives DNA replication, nuclear envelope breakdown, spindle assembly and congression of chromosomes to the metaphase plate. Local degradation of CycB at the spindle drives chromosome segregation and nuclear envelope reformation. Simulations of the model agree with salient features of wild-type embryos, as summarized in Figure 7 of Edgar *et al* (1994b) and our Figure 3. Wild-type embryos arrest in interphase of cycle 14, but mutant embryos may arrest sooner or later (or may not cycle at all), depending on their genetic make-up. The model is consistent with these subtle effects on nuclear division cycles, as summarized in Table III. Lastly, we have shown that the model accounts for differential effects of alpha-amanitin treatment before and after cycle 6.

Our model does not attempt to describe the complex regulatory signals introduced at the mid-blastula transition, when many zygotic genes are newly transcribed.

Some general principles drawn from the model

Roles of positive and negative feedback

The delayed negative-feedback circuit involving Fzy/APC and MPF is primarily responsible for controlling the early nuclear divisions. By contrast, the positive-feedback circuits, involving

MPF, Wee1 and String, are not essential to the early mitotic cycles and play important roles only late in the syncytial phase, contributing to the maintenance of large amplitude oscillations and reliable interphase arrest in cycle 14. Even in the absence of Wee1, the model predicts rather normal looking cycles (see Supplementary Figure 2), which arrest because the embryo runs out of CycB. On closer examination, the cycles are faster than normal and disappear by damped oscillations in MPF activity. The actual number of cycles observed under these conditions is difficult to predict, as discussed previously.

Role of the unreplicated-DNA checkpoint

The first 6 cycles of the *Drosophila* embryo are extremely short ($\sim$10 min), then cycles 7–13 get progressively longer (up to $\sim$20 min). This lengthening of the mitotic cycle could be due in part to the reduction of CycB level in the embryo and in part to the 'DNA replication' checkpoint, which delays MPF activation while DNA is being replicated. For $N=2^{C-1}<64$, N in the embryo is too small to have removed much CycB or to generate much of an unreplicated-DNA signal. For cycles 7–10, the lengthening of cycle time is attributable to CycB reduction only (Ji *et al*, 2004; Crest *et al*, 2007), as can be established using embryos with different dosages of *cycB* with or without *grapes*. (The *grapes* gene encodes Chk1 kinase (Sibon *et al*, 1997). In response to unreplicated DNA, Chk1 phosphorylates String, which causes String to be sequestered in the cytoplasm (Lopez-Girona *et al*, 1999).) Cycles 11–13, on the other hand, are lengthened by a combination of CycB depletion and the unreplicated-DNA checkpoint.

Our model (Figure 3) shows modest lengthening of late mitotic cycles due to CycB depletion and Wee1-dependent phosphorylation of MPF. We can easily introduce a DNA replication checkpoint into the model by increasing the value of k_{outs} when DNA is unreplicated. The increase should depend on N and should be periodic during normal cycling and steady during a sustained block to DNA replication. Simulations (Supplementary Figure 3) confirm that proper lengthening of mitotic cycles 11–13 depend on engaging the DNA replication checkpoint.

Roles of nuclear transport of regulatory proteins

To get robust interphase arrest in cycle 14 of wild-type embryos, it is important that MPF be targeted to the nuclear compartment. In our calculations, $k_{out}=0$ for MPF; if $k_{out}>0.1$, then an extra cycle is observed. In addition, Wee1 must accumulate in the nucleus ($k_{in}=5\times k_{out}$ for Wee1 transport, in our simulations); if $k_{in}=k_{out}$ for Wee1, then the cell proceeds through 14 cycles instead of 13. On the other hand, String need not be differentially transported across the nuclear boundary ($k_{in}=k_{out}$ for String transport, in our simulations). String may be targeted to the cytoplasm; the model works quite well even with $k_{in}=0$ for String.

Some predictions

Rate constants

In fitting the model to the behavior of wild-type and mutant embryos, we have had to assign specific values to the reaction rate constants and transport coefficients in the model. These values are constrained by the available data and represent predictions of the model. Although tedious, it is possible to obtain direct experimental evidence for some of these kinetic constants, to test the predictive power of the model. In a similar situation years ago, we predicted the rate constants of the MPF-APC-Wee1-Cdc25 control system in *Xenopus* embryos (Novak and Tyson, 1993), and these predictions were born out by subsequent measurements of the phosphorylation and dephosphorylation of recombinant proteins in frog egg extracts (Kumagai and Dunphy, 1995; Marlovits *et al*, 1998; Zwolak *et al*, 2005).

Mutants

The model can be used to predict the phenotype of any mutant that can be constructed by knocking down and/or overexpressing any of the genes encoding components of the regulatory mechanism. For example, of the mutants described in Table III, some of the Fzy and Wee1 mutants have yet to be characterized experimentally.

Nuclear envelope breakdown

The nuclear 'compartments' of the model are localized regions around chromosomes and spindles where MPF activity can periodically build up and be destroyed, thereby governing nuclear division cycles without perturbing much the cytoplasmic 'compartment' until there are 1000's of nuclei in the egg. In our model, we allow transport of proteins (MPF, Wee1 and String) between these compartments, but we do not change the transport coefficients during the phase of the division cycle when the nuclear envelope is disassembled. In the crowded environment of the cell for the few minutes when the nuclear envelope is missing, protein movements between spindle environs and bulk cytoplasm may still be restricted, but we may certainly expect intercompartmental transport to be faster than when the nuclear envelope is intact. To study the effects of increased rates of protein transport between nuclear and cytoplasmic compartments when the nuclear envelope is missing, we created an alternative version of the model, as described in the 'ode' file in the Supplementary Material. Briefly put, we assign two different values to each transport coefficient (k_{in} and k_{out} for MPF, Wee1 and String): a 'small' value when the nuclear envelope is intact and a 'large' value when the nuclear envelope is disassembled. We call this the 'nuclear envelope breakdown'—NEB—model.) For Wee1 and String, we assume that

$$k_{outw,large}=k_{inw,large}=f_w\times k_{inw,small}, \text{ and } k_{outs,large}=k_{ins,large}=f_s\times k_{ins,small,}$$

with an adjustable factor $f>1$ for each species. For MPF, as $k_{outm,small}=0$, we assume that

$$k_{inw,large}=f_m\times k_{inm,small}, \text{ and } 0<k_{outm,large}/k_{inm,large}\ll 1.$$

The latter inequality seems appropriate, because MPF dimers are likely bound to mitotic spindles, so they are not easily lost from the nuclear compartment even when the nuclear envelope breaks down. We assume that the nuclear envelope is disassembled when MPF activity is greater than some

threshold. (In principle, the thresholds for nuclear envelope breakdown and re-assembly could be different. We set the thresholds so that the nuclear envelope is missing for about 30% of the mitotic cycle.)

With the 'NEB' version of the differential equations, we can test how sensitive the model is to variations in transport rates before and after nuclear envelope breakdown. Reassuringly, we find that Figure 3 is not much changed over a range of f values >1 (see, for example, Supplementary Figure S4). As expected, f_m is most restricted; if $f_m > 2.5$, then the cycle blocks in M-phase. Furthermore, if $k_{outm,large}$ is too large (say, $> k_{inm,large}$), then [MPF_n] starts dropping as soon as the nucleus enters mitosis. For this reason, we suppose that nuclear MPF is bound to a structure during mitosis (e.g., the spindle) so that it cannot interchange freely with the cytoplasmic pool. On the other hand, String and Wee1 may move freely between nuclei and cytoplasm during M-phase (acceptable behavior is observed for f_s and f_w as large as 10).

Conclusion

Systematic comparison of mathematical models of the networks controlling cell division cycles in various organisms helps to delineate common principles as well as significant variations in the design of these networks along the evolutionary tree (Csikasz-Nagy *et al*, 2006). The model presented here of the syncytial mitotic cycles in *Drosophila* embryos is closely related to earlier models covering cell cycle regulation in frog eggs (Novak and Tyson, 1993)and fission yeast cells (Novak and Tyson, 1995). In contrast to those models, the *Drosophila* model underscores the importance of nuclear compartmentation of cyclin degradation to achieve very rapid multiplication of nuclei in the fruit fly embryo. The record-setting pace of nuclear division presumably helps the developing fruit fly to proceed as rapidly as possible through the most vulnerable stage of its life cycle.

Methods

Programs and software

The models are defined in terms of ordinary differential equations and simulated with the software XPPAut (http://www.math.pitt.edu/~bard/xpp/xpp.html) (Ermentrout, 2002). An 'ode' file for simulating Figure 3 is provided in the Supplementary Material. To compute Figure 1B, some numerical constants must be changed, as described in the ode file. When modified as described therein, the ode file can also implement the NEB model described in the Discussion. A second ode file is supplied for computing bifurcation diagrams (as in Figure 2) using XPPAut. In addition, our model is available as an SBML file from the BioModels database (http://www.ebi.ac.uk/biomodels, temporary accession MODEL1509031628).

Rescaling of concentrations after division

Define X_{n_before} and X_{c_before} to be the concentrations of species X in the nucleus and in the cytoplasm before nuclear division (at time t), and X_{n_after} and X_{c_after} to be the concentrations after division (at time $t+\Delta t$). Then:

$$X_{Total\_before} = (1 - N_{before}\varepsilon)X_{c\_before} + N_{before}\varepsilon X_{n\_before}$$

$$X_{Total\_after} = (1 - N_{after}\varepsilon)X_{c\_after} + N_{after}\varepsilon X_{n\_after}$$

$$N_{after} = 1.95N_{before}$$

Insisting that $X_{Total\_after=}X_{Total\_before}$, we find that X_{n_after} and X_{c_after} must be adjusted at nuclear division as follows:

$$X_{c\_after} = \frac{1 - N_{before}\varepsilon}{1 - 1.95N_{before}\varepsilon}X_{c\_before}$$

$$X_{n\_after} = \frac{X_{n\_before}}{1.95}$$

This rescaling needs to be applied to MPF, Wee1 and String each time the nuclei divide.

Supplementary information

Supplementary information is available at the *Molecular Systems Biology* website (www.nature.com/msb).

Acknowledgements

This work has been supported by grants from the Defense Advanced Research Project Agency (AFRL No. F30602-02-0572), the James S. McDonnell Foundation (21002050), the European Commission (LSHG-CT-2004-503568) and the *Action de Recherche Concertée* INRIA MOCA (2006).

References

Bashirullah A, Halsell SR, Cooperstock RL, Kloc M, Karaiskakis A, Fisher WW, Fu W, Hamilton JK, Etkin LD, Lipshitz HD (1999) Joint action of two RNA degradation pathways controls the timing of maternal transcript elimination at the midblastula transition in *Drosophila melanogaster*. *EMBO J* **18:** 2610–2620

Crest J, Oxnard N, Ji JY, Schubiger G (2007) Onset of the DNA replication checkpoint in the early *Drosophila* embryo. *Genetics* **175:** 567–584

Csikasz-Nagy A, Battogtokh D, Chen KC, Novak B, Tyson JJ (2006) Analysis of a generic model of eukaryotic cell-cycle regulation. *Biophys J* **90:** 4361–4379

Dawson IA, Roth S, Akam M, Artavanis-Tsakonas S (1993) Mutations of the fizzy locus cause metaphase arrest in *Drosophila melanogaster* embryos. *Development* **117:** 359–376

Dawson IA, Roth S, Artavanis-Tsakonas S (1995) The *Drosophila* cell cycle gene fizzy is required for normal degradation of cyclins A and B during mitosis and has homology to the CDC20 gene of *Saccharomyces cerevisiae*. *J Cell Biol* **129:** 725–737

Edgar BA, Datar SA (1996) Zygotic degradation of two maternal Cdc25 mRNAs terminates *Drosophila*'s early cell cycle program. *Genes Dev* **10:** 1966–1977

Edgar BA, Lehman DA, O'Farrell PH (1994a) Transcriptional regulation of string (cdc25): a link between developmental programming and the cell cycle. *Development (Cambridge, England)* **120:** 3131–3143

Edgar BA, O'Farrell PH (1990) The three postblastoderm cell cycles of *Drosophila* embryogenesis are regulated in G2 by string. *Cell* **62:** 469–480

Edgar BA, Sprenger F, Duronio RJ, Leopold P, O'Farrell PH (1994b) Distinct molecular mechanism regulate cell cycle timing at successive stages of *Drosophila* embryogenesis. *Genes Dev* **8:** 440–452

Ermentrout B (2002) *Simulating, Analyzing, and Animating Dynamical Systems: A guide to XPPAUT for Research and Students*. Soc for Industrial & Applied Math: Philadelphia, USA

Felix MA, Labbe JC, Doree M, Hunt T, Karsenti E (1990) Triggering of cyclin degradation in interphase extracts of amphibian eggs by cdc2 kinase. *Nature* **346:** 379–382

Gerhart J, Wu M, Kirschner M (1984) Cell cycle dynamics of an M-phase-specific cytoplasmic factor in *Xenopus laevis* oocytes and eggs. *J Cell Biol* **98:** 1247–1255

Glotzer M, Murray AW, Kirschner MW (1991) Cyclin is degraded by the ubiquitin pathway. *Nature* **349:** 132–138

Hara K, Tydeman P, Kirschner M (1980) A cytoplasmic clock with the same period as the division cycle in *Xenopus* eggs. *Proc Natl Acad Sci USA* **77:** 462–466

Huang J, Raff JW (1999) The disappearance of cyclin B at the end of mitosis is regulated spatially in *Drosophila* cells. *EMBO J* **18:** 2184–2195

Huang JY, Raff JW (2002) The dynamic localisation of the *Drosophila* APC/C: evidence for the existence of multiple complexes that perform distinct functions and are differentially localised. *J Cell Sci* **115:** 2847–2856

Jaeger J, Blagov M, Kosman D, Kozlov KN, Manu, Myasnikova E, Surkova S, Vanario-Alonso CE, Samsonova M, Sharp DH, Reinitz J (2004) Dynamical analysis of regulatory interactions in the gap gene system of *Drosophila melanogaster*. *Genetics* **167:** 1721–1737

Ji JY, Squirrell JM, Schubiger G (2004) Both cyclin B levels and DNA-replication checkpoint control the early embryonic mitoses in *Drosophila*. *Development* **131:** 401–411

Kumagai A, Dunphy WG (1995) Control of the Cdc2/cyclin B complex in Xenopus egg extracts arrested at a G2/M checkpoint with DNA synthesis inhibitors. *Mol Biol Cell* **6:** 199–213

Lopez-Girona A, Furnari B, Mondesert O, Russell P (1999) Nuclear localization of Cdc25 is regulated by DNA damage and a 14-3-3 protein. *Nature* **397:** 172–175

Marlovits G, Tyson CJ, Novak B, Tyson JJ (1998) Modeling M-phase control in *Xenopus* oocyte extracts: the surveillance mechanism for unreplicated DNA. *Biophys Chem* **72:** 169–184

Morgan DO (2007) *The Cell Cycle: Principles of Control*. London: New Science Press Ltd

Myers FA, Francis_Lang H, Newbury SF (1995) Degradation of maternal string mRNA is controlled by proteins encoded on maternally contributed transcripts. *Mech Dev* **51:** 217–226

Novak B, Tyson JJ (1993) Numerical analysis of a comprehensive model of M-phase control in *Xenopus* oocyte extracts and intact embryos. *J Cell Sci* **106** (Part 4)**:** 1153–1168

Novak B, Tyson JJ (1995) Quantitative analysis of a molecular model of mitotic control in fission yeast. *J Theor Biol* **173:** 283–305

Peters JM (2006) The anaphase promoting complex/cyclosome: a machine designed to destroy. *Nat Rev Mol Cell Biol* **7:** 644–656

Raff JW, Jeffers K, Huang JY (2002) The roles of Fzy/Cdc20 and Fzr/Cdh1 in regulating the destruction of cyclin B in space and time. *J Cell Biol* **157:** 1139–1149

Sanchez L, Thieffry D (2003) Segmenting the fly embryo: a logical analysis of the pair-rule cross-regulatory module. *J Theor Biol* **224:** 517–537

Sibon OC, Stevenson VA, Theurkauf WE (1997) DNA-replication checkpoint control at the *Drosophila* midblastula transition. *Nature* **388:** 93–97

Stumpff J, Duncan T, Homola E, Campbell SD, Su TT (2004) *Drosophila* Wee1 kinase regulates Cdk1 and mitotic entry during embryogenesis. *Curr Biol* **14:** 2143–2148

Su TT, Sprenger F, DiGregorio PJ, Campbell SD, O'Farrell PH (1998) Exit from mitosis in *Drosophila* syncytial embryos requires proteolysis and cyclin degradation, and is associated with localized dephosphorylation. *Genes Dev* **12:** 1495–1503

Tyson JJ, Csikasz-Nagy A, Novak B (2002) The dynamics of cell cycle regulation. *Bioessays* **24:** 1095–1109

von Dassow G, Meir E, Munro EM, Odell GM (2000) The segment polarity network is a robust developmental module. *Nature* **406:** 188–192

Wolpert L (2001) *Principles of Development*. Oxford University Press: Oxford

Zwolak JW, Tyson JJ, Watson LT (2005) Parameter estimation for a mathematical model of the cell cycle in frog eggs. *J Comput Biol* **12:** 48–63